

Amazon estuary – assessment of trace elements in seabed sediments

L. B. L. S. Lara, E. A. N. Fernandes, H. Oliveira, M. A. Bacchi, E. S. B. Ferraz

Centro de Energia Nuclear na Agricultura – CENA/USP, Laboratório de Radioisótopos, CP 96 13400-970 Piracicaba SP, Brazil

(Received June 20, 1996)

The interactive processes operating on the continental shelf adjacent to the river mouth control the amount and the characteristics of the Amazon discharge reaching the Atlantic Ocean. In this study, the distribution of trace elemental concentrations, with emphasis to the rare-earth elements, in sediment cores collected at several stations from the Amazon continental shelf during the falling water period was investigated by instrumental neutron activation analysis. Cores from the terrigenous and blue water zones have relatively uniform REE concentrations throughout the profile. Cerium anomalies for samples of the upper section of the eight stations are consistently positive and of high values (normally > 2). Similar variation in the elemental concentration ratios between the seabed sediments and Amazon River suspended sediments was seen for stations located in the biogenic and blue water zones, with an enrichment for Ce, Sm, Fe, Th, and Sc and a depletion for the La, Eu, Tb, Yb, Co, Cr, Cs, Hf, Ta, and Zn. The shale-normalized REE patterns from shelf sediments are enriched in LREE relative to HREE, with enrichment factors varying from 1.5 for stations near the river mouth (terrigenous zone) to 1.9 for stations located far in the blue water zone. Published data for the Amazon River suspended sediment agree remarkably well with this observation of LREE-enrichment.

Introduction

The Amazon River, the largest river in the world in terms of water discharge ($6 \cdot 10^{15} \text{ l} \cdot \text{y}^{-1}$)¹ and drainage basin area ($7 \cdot 10^6 \text{ km}^2$)², is responsible for about 80% of the total amount of sediment particles deposited in the equatorial zone of the Atlantic Ocean.¹ This major dispersal system annually transports to a complex marine environment approximately $1.2 \cdot 10^9$ tons of sediment derived from the Andes, composed primarily (85–95%) of silt and clay-sized particles.^{4,5} Before the deposition on the shelf, these particles undergo chemical weathering during their cycle of transport and storage in the Amazon River system. The maximum sediment discharge occurs just prior to maximum water discharge (May and June) and is about 6 times greater than the minimum sediment discharge (October and November).⁵

The Amazon is discharged as a freshwater plume into the ocean flowing over the more dense seawater and extending for many hundreds of kilometers, transporting most of the sediment directly into the ocean rather than allowing coagulation and deposition in the estuary.³ Circulation on the Amazon shelf is influenced by the interaction of this freshwater plume with strong tidal currents (with speeds higher than $10 \text{ cm} \cdot \text{s}^{-1}$ at 1 m above the shelf bottom) and the northwestward flowing North Brazilian Coastal Current (NBCC), being responsible for the mixture of sediments that occurs at water depth approximately 30 m above the seabed.⁵ Of the sediment discharged by the Amazon River, half is accumulated on the shelf and the remainder is dispersed into the Atlantic Ocean.⁴

The Amazon estuary can be divided into three broad zones based upon the color and type of particles in the surface water.^{7,8} A terrigenous zone in the low salinity region is characterized by brown muddy water rich in suspended particles from the river and also resuspended shallow sediments. This zone gives way to a biogenic zone of high productivity at intermediate salinities, and the blue water zone, with the lowest total particle concentration.

Processes acting on the Amazon shelf greatly influence the particulate and dissolved loads reaching the Atlantic Ocean. Trace elements undergo different types of chemical reactions during the mixing of river water and seawater in estuaries. Estuarine reactions play an important role in establishing the oceanic composition of the rare-earth elements (REEs) and in linking the REE geochemistries of continental waters and ocean water.⁹

Because of their chemical behavior, complex formation and oxidation–reduction reactions,^{10, 11} numerous geochemical studies have been performed on the relative abundances of the rare earth elements in terrestrial and aquatic systems.^{12–14} Even with these characteristics, fractionation of REE, i.e. changes in relative abundance among the series, may occur during geochemical reactions at low temperatures in soils, fluvial and estuarine waters.^{9, 15} There is a systematic reduction of the ionic radii of the trivalent REEs, from La (the lightest REE) to Lu (the heaviest REE). Because of this lanthanide contraction, changes are noted in the complex formed by the REEs with their respective ligands. The extension of the fractionation between the change of the sites of surface particles in the solution ligands depends on the different

affinities or even competitiveness between these REE phases.¹⁶⁻¹⁸

Rare earth elements in the trivalent form behave as a coherent group, although two elements, Ce and Eu, may exhibit anomalies due to changes in their oxidation states.¹⁵ While Ce(III) has a solution chemistry similar to its trivalent neighbours, its oxidation to Ce(IV) results in the formation of a less soluble ion,⁹ leading to anomalous distribution when compared with other REE. The extent to which Ce is fractionated can be quantified by the Ce anomaly, which is a measure of the Ce abundance observed to that expected for its trivalent form.⁹ Ce anomalies have been observed particularly within the ocean basins,¹⁵ where seawater is normally depleted in Ce by comparison with neighbouring La and Nd⁹ and an enrichment is seen in seabed sediments.^{14,19} Trace elements like As, Cu, Fe, I, Mn, Sb and Se are also affected by their multiple oxidation states in these environments.¹⁵

This approach aimed at presenting new data on the trace element distributions, especially the REEs, in the seabed sediments from the Amazon continental shelf. A comparison of the results with data obtained previously from the Amazon River suspended sediment²⁰ can provide information on the geochemical behavior of this important group of elements and shed new light for further studies in this interdisciplinary project.

Experimental

This paper is related with the participation of CENA in the Project AmasSeds – A Multidisciplinary Amazon Shelf Sediment Study, performed during the period of falling water discharge (Cruise IV, Leg 3, November 5–13, 1991), aboard the ship RV Columbus Iselin (University of Miami, USA) departing from the port of Belém, PA, Brazil. Sediment samples from the upper 50 cm of the seabed were collected at several stations from the Amazon continental shelf (between the river mouth and about 4 °N)

Table 1. Location of sampling stations in the study area

Sample No.	Pressure (d-bars)	Salinity ‰	Light, %	Latitude	Longitude
AMS4308	64.0	36.555	88.80	1°10.42'N	48°12.06'W
AMS4311	11.0	22.492	0.00	0°43.89'N	48°32.40'W
AMS4315	7.0	18.882	0.40	1°39.28'N	49°11.78'W
AMS4318	18.0	36.422	51.30	2°04.31'N	48°52.56'W
AMS4328	17.0	33.161	61.20	2°28.78'N	49°11.43'W
AMS4333	16.0	32.261	0.00	2°46.64'N	49°45.73'W
AMS4345	23.0	35.950	1.30	3°11.74'N	50°06.38'W
AMS4349	14.0	35.757	37.60	4°02.98'N	50°55.89'W

using a box corer. A map showing the location of stations can be found in Fig. 1. Table 1 shows the pressure, salinity, light and coordinates of sample collection in the Northwest Atlantic Ocean. The same AMS sample identification numbers have been used in this paper.

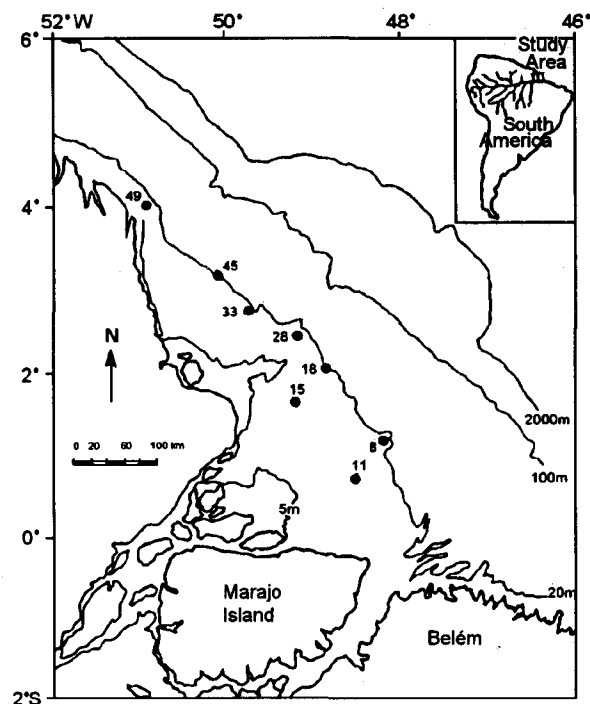


Fig. 1. Location map of stations utilized in this study of the Amazon continental shelf

Samples were brought to CENA (Centro de Energia Nuclear na Agricultura, Piracicaba, SP) where they were oven-dried at 60 °C, ground in a synerized alumina-lined disk mill and sieved for separation of particle size below than 53 µm. Sediments were analyzed for their trace element concentrations by instrumental neutron activation analysis. Subsamples of about 100 mg of the < 53 µm fraction were inserted into special polyethylene containers, which were surrounded by Ni–Cr wire flux monitor. Samples and standard reference materials (SD-M-2/TM and SL-1) were irradiated for about 7 hours with a thermalized neutron flux of $5 \cdot 10^{12} \text{ n} \cdot \text{cm}^{-2} \cdot \text{s}^{-1}$ at the IEA-R1 research reactor of IPEN (Instituto de Pesquisas Energéticas e Nucleares, São Paulo). Irradiated samples were returned to CENA for the induced radioactivity measurements with a HP Ge detector coupled to a multi-channel buffer and spectral analysis system.

Environmental parameters like salinity, light, and depth were obtained from the AmasSeds' data bank.

Results and discussion

Rare earth concentrations were normalized by a set of shale concentrations representing an average of North American, European, and Russian shale composites which have been used in the majority of recent publications on REE marine geochemistry.¹⁴ Another set of shale REE concentrations, the PAAS (Post Archean average Australian Shale), was also adopted in this study as large differences can result when using distinct normalizations.

Concentrations of La, Ce, Nd, Sm, Eu, Tb, Yb, and Lu and their respective shale-normalized ratios found for the surface sediments (to a depth of 2–5 cm) from eight stations in the shelf and for suspended solids collected along 1800 km of the Amazon River, from Santarém to Óbidos (700 km upstream the river mouth),²⁰ are given in Table 2. For this paper La, Ce, Nd, and Sm represent the light (LREE), Eu and Tb the middle (MREE), and Yb and Lu the heavy (HREE) rare earth elements.¹⁴ Figure 2 shows the normalization patterns of sediments in stations 15, 08, and 49, located into the terrigenous, biogenic and blue water zones, respectively. It can be seen from the figure that the shale-normalized rare-earth element patterns of seabed sediments are enriched in LREE relative to HREE. The PAAS/shale ratios vary considerably across the REE series, the LREE in PAAS are significantly enriched over HREE with respect to shale.¹⁴ Comparison of the shale- and PAAS-normalizations indicates a pattern deviation with higher normalized ratios for PAAS.

The term LREE enrichment factor has been defined as equal to the La shale-normalized ratio divided by Lu shale-normalized ratio.¹⁴ For station 15, the nearest to the river mouth, the normalized ratio decreases from 1.27 for La down to 0.83 for Lu, with an enrichment factor equal to 1.5. For station 08, the ratio decreases from 1.30 for La

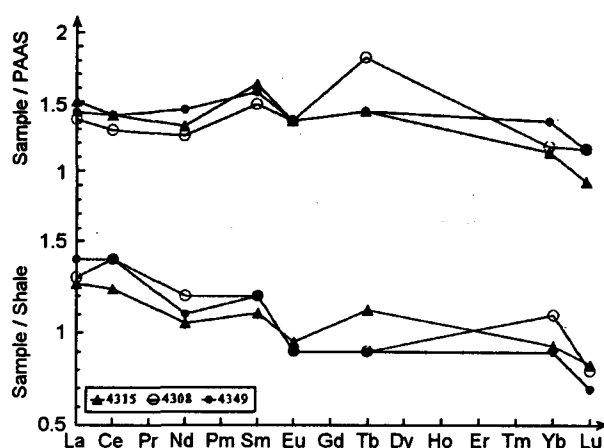


Fig. 2. REE patterns of shale and PAAS-normalized ratios for seabed (2–5 cm) sediments of stations 15, 08 and 49

down to 0.84 for Lu, with enrichment factor equal to 1.6, and for station 49, from 1.43 to 0.69, with enrichment factor equal to 2.0. Suspended solid samples from the Amazon River²⁰ also present an enrichment of 1.7 (in agreement with a literature value of 1.8¹⁴) for the LREE in comparison with HREE, quantified by using the La_n/Yb_n ratio (where n indicates the normalization), since there is no Lu concentration reported.²⁰

As seen in Table 2, the enrichment factors for LREE in all stations are consistently higher than unity, with enrichment factors ranging from 1.3 to 2.1, with an average of 1.6. This fact denotes a fractionation of the rare earth elements in the Amazon estuary, suggesting that the preferential removal of the heavy REE followed by the middle and light REE takes place in the estuarine region as a whole.

Table 2. Concentration (in ppm) of REE and shale-normalized ratios in seabed sediments of 2–5 cm horizon at eight stations

Station	Concentration, ppm								Shale-normalized values							
	La	Ce	Nd	Sm	Eu	Tb	Yb	Lu	La	Ce	Nd	Sm	Eu	Tb	Yb	Lu
4318	60.5	130	59.8	8.1	1.9	1.2	4.7	0.7	1.5	1.6	1.6	1.1	1.2	1.0	1.3	1.2
4345	49.3	106	47.0	6.6	1.6	0.8	3.0	0.5	1.2	1.3	1.2	0.9	1.0	0.6	0.8	0.7
4328	47.2	85.9	37.9	7.7	1.4	1.0	3.6	0.6	1.2	1.0	1.0	1.0	0.9	0.8	1.0	0.9
4308	53.9	112	46.2	8.8	1.5	1.1	3.8	0.5	1.3	1.4	1.2	1.2	0.9	0.9	1.1	0.8
4311	49.6	105	42.1	8.1	1.5	1.4	3.6	0.5	1.2	1.3	1.1	1.1	0.9	1.1	1.0	0.9
4315	51.9	103	40.0	8.3	1.5	1.4	3.3	0.5	1.3	1.2	1.1	1.1	0.9	1.1	0.9	0.8
4349	56.2	112	43.4	9.1	1.5	1.1	3.2	0.4	1.4	1.4	1.1	1.2	0.9	0.9	0.9	0.7
4333	62.1	103	47.7	8.5	1.6	0.9	2.8	0.4	1.5	1.2	1.3	1.1	1.0	0.7	0.8	0.7
SS*	51.5	84.9		8.0	1.7	1.3	3.9		1.3	1.0		1.1	1.0	1.1	0.7	
Shale**	41.0	83.0	38.0	7.5	1.6	1.2	3.5	0.6								

*REE concentration in Amazon River suspended sediment.²⁰

**REE concentration (in ppm) in shale used for normalization.

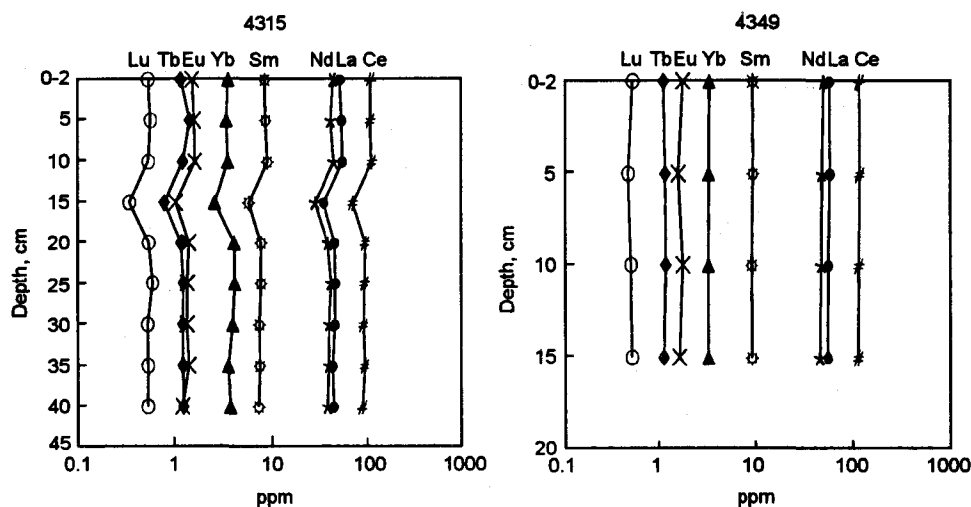


Fig. 3. Vertical profiles of REE in seabed sediments of stations 15 and 49

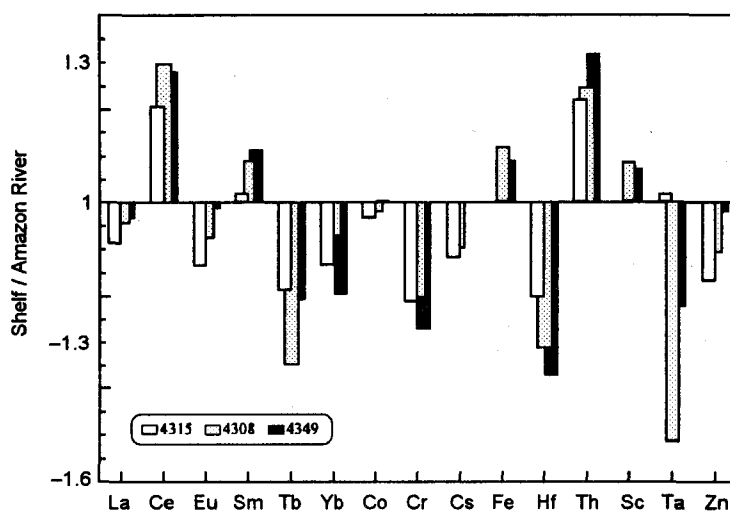


Fig. 4. Elemental concentration ratios between seabed sediments of stations 15, 08 and 49 and suspended sediments from Amazon River

The highest LREE enrichment factors were found for the stations 33 (2.1) and 49 (2.0), both located into the blue water zone, but with high turbidity near to the seabed because of the resuspension of sediments associated with tidal currents. On the other hand, the lowest enrichment factors (1.2 and 1.3) were observed for stations 18 and 28, also in the blue water zone, but presenting lower turbidity values compared with 33 and 49.

The PAAS-normalized patterns of surface sediments (2–5 cm horizon) from cores 08, 15, and 49 (Fig. 2) denote that the LREE have relatively constant ratios, with variations beginning from the intermediate REE, the main feature of the Amazon estuary.^{6,17}

In surface water, Ce^{3+} released from particles will oxidize and so be removed relative to its trivalent neighbours. In deep sea sediments, this same reaction means that Ce released from decomposing particles will be less mobile than the REE^{+3} (this is observed in terms of the positive Ce anomaly).²¹ Ce anomalies observed for samples of the upper section (2–5 cm) are consistently positive with high values (normally > 2), indicating an accumulation due to the insolubility of Ce(IV). This fact emphasizes the assumption that in water and suspended solid samples from marine environment Ce anomaly is frequently negative, since its trivalent state is not observed.⁹ Altering the oxidation state to Ce(IV), the element becomes less soluble and removed from water

Table 3. Concentration (in ppm, Fe in %) of elements in seabed sediments of 2–5 cm horizon at eight stations in the shelf and in the Amazon River suspended sediment

Element	4311	4315	4318	4308	4328	4333	4345	4349	SS ²⁰
Ce	108.2	102.5	112.7	110.2	72.6	98.6	109.3	108.7	84.9
Co	18.2	18.1	19.3	18.5	10.2	1.9	19.8	18.9	18.8
Cr	77.4	75.9	128.3	77.0	42.9	72.9	81.7	70.4	96.3
Cs	10.1	9.9	9.2	10.1	1.7	10.4	12.4	11.2	11.2
Eu	1.6	1.5	1.7	1.6	1.1	1.6	1.6	1.7	1.7
Fe	4.5	4.4	4.9	4.9	3.9	4.9	5.4	4.8	4.4
Hf	6.2	5.8	11.3	4.9	12.5	5.1	3.9	4.5	7.2
La	47.3	46.5	40.2	48.9	30.9	44.8	37.9	19.4	51.1
Sc	16.8	16.6	16.2	18.1	8.1	17.8	19.4	17.8	16.7
Sm	8.6	8.1	7.2	8.7	6.2	8.2	6.9	8.9	7.9
Ta	1.8	1.3	1.4	0.6	0.7	1.5	2.2	1.0	1.3
Tb	1.47	1.1	0.9	0.9	0.6	0.9	0.9	1.1	1.3
Th	14.1	14.3	16.6	14.6	9.1	15.0	17.2	15.4	11.7
Yb	3.7	3.4	4.1	3.6	2.5	3.4	3.3	3.2	3.9
Zn	117.8	119.6	123.5	128.8	65.5	129.7	109.8	141.2	144.0

column to precipitate into the seabed sediments, promoting its accumulation in the water-sediment interface. The greatest Ce normalized ratio was found for station 18, in which a high salinity is observed (Table 1).

Figure 3 shows the depth profiles of the REE concentrations in sediment cores of stations 15 and 49. Station 15 is located in a region of high turbulence caused by the confluence of Amazon River and Atlantic Ocean. The low salinity suggests that the behavior of the elements is influenced by the sediments transported by the river, as well as the small light percentage that pass through the water column depicts high concentration of suspended solids. Because of its location in the Amazon delta, at the north canal, this station is more likely influenced by the river. Nevertheless, uniform REE concentrations were found throughout its 40 cm length, including the consistent concentration gradient exhibited between 10 and 20 cm. Similar uniform concentration distribution pattern is shown for the station 49, the farthest station studied in relation to the mouth, which reinforces the coherence of REE chemical behavior even in such dynamic environment.

Figure 4 compares the elemental concentration ratios between seabed sediments for stations 15 (terrigenous zone), 08 (biogenic zone), and 49 (blue water zone) and suspended sediments from the Amazon River.²⁰ It can be seen that Fe content in station 15 approaches that of the river (Table 3), while Ta and Sc are very different for the other stations. Sc concentration is higher for the river samples, while Ta is enriched in the shelf.

Stations located in the biogenic and blue water zone show the same variation. There is an enrichment of Ce, Sm, Fe, Th, and Sc and a depletion for the La, Eu, Tb, Yb, Co, Cr, Cs, Hf, Ta, and Zn, except for the higher Co concentration found in seabed sediments of station 49.

The continental shelf near the mouth of a major river is characterized by the existence of large gradients in environmental parameters like salinity, high concentration of suspended solids, particle and solution chemistry.²² In spite of this, a consistent spatial and temporal trace elemental distribution was verified in all sediment cores taken in the three broad zones (blue water, biogenic and terrigenous) studied in the Amazon continental shelf.

*

The authors are grateful to the Project AmasSeds Brazilian Coordinator, Prof. Alberto FIGUEIREDO, Universidade Federal Fluminense, Niterói, RJ, for the unique opportunity of participating on this joint research, and for the sampling facilities offered. Thanks are also due to CNPq – Conselho Nacional de Desenvolvimento Científico e Tecnológico and FAPESP – Fundação de Amparo à Pesquisa do Estado de São Paulo for the financial support.

References

1. R. H. MEADE, C. F. NORDIN, W. F. CURTIS, F. M. C. RODRIGUES, C. M. DOVALE, J. M. EDMOND, *Nature*, 178 (1979) 161.
2. R. J. GIBBS, *Geochim. Cosmochim. Acta*, 36 (1972) 1061.
3. R. J. GIBBS, L. KONWAR, *Continental Shelf Res.*, 6 (1986) 127.
4. C. A. NITTROUER, D. J. DEMASTER, *Continental Shelf Res.*, 6 (1986) 5.
5. R. H. MEADE, T. DUNE, J. E. RICHEY, U. M. SANTOS, E. SALATI, *Science*, 228 (1985) 488.
6. S. A. KUEHL, D. J. DEMASTER, C. A. NITTROUER, *Continental Shelf Res.*, 6 (1986) 365.
7. J. D. MILLIMAN, E. BOYLE, *Science*, 189 (1975) 995.
8. E. R. SHOLKOVITZ, N. B. PRICE, *Geochim. Cosmochim. Acta*, 44 (1980) 163.
9. E. R. SHOLKOVITZ, *Geochim. Cosmochim. Acta*, 57 (1993) 2181.
10. K. J. CANTRELL, R. H. BYRNE, *Geochim. Cosmochim. Acta*, 51 (1987) 597.

11. H. ELDERFIELD, R. UPSTILL-GODDARD, E. R. SHOLKOVITZ, *Geochim. Cosmochim. Acta*, 54 (1990) 971.
12. J. M. MARTIN, J. M. O. HOGDAHL, J. C. PHILIPPOT, *J. Geophys. Res.*, 81 (1976) 3119.
13. H. J. W. DE BAAR, M. P. BACON, P. G. BREWER, *Nature*, 301 (1983) 324.
14. E. R. SHOLKOVITZ, *Am. J. Sci.* 288 (1988) 236.
15. H. J. W. DE BAAR, M. P. BACON, P. G. BREWER, K. W. BRULAND, *Geochim. Cosmochim. Acta*, 49 (1985) 1943.
16. D. R. TURNER, M. WHITFIELD, A. G. DICKSON, *Geochim. Cosmochim. Acta*, 45 (1981) 855.
17. R. H. BYRNE, K. H. KIM, *Geochim. Cosmochim. Acta*, 54 (1990) 2645.
18. Y. EREL, J. J. MORGAN, *Geochim. Cosmochim. Acta*, 55 (1991) 1807.
19. E. R. SHOLKOVITZ, *Chem. Geol.*, 88 (1990) 337.
20. E. S. B. FERRAZ, E. A. N. FERNANDES, *J. Radioanal. Nucl. Chem.*, (1995).
21. H. ELDERFIELD, M. J. GREAVES, *Nature*, 296 (1982) 214.
22. B. A. MCKEE, D. J. DEMASTER, C. A. NITTROUER, *Continental Shelf Res.*, 6 (1986) 87.